AMERICAN SOCIETY FOR MICROBIOLOGY | Journal of Virology

Structure-Function Analysis of the ϕX174 DNA-Piloting Protein Using Length-Altering Mutations

Aaron P. Roznowski, Bentley A. Fane

The BIO5 Institute, University of Arizona, Tucson, Arizona, USA

ABSTRACT

Although the ϕX174 H protein is monomeric during procapsid morphogenesis, 10 proteins oligomerize to form a DNA translocating conduit (H-tube) for penetration. However, the timing and location of H-tube formation are unknown. The H-tube's highly repetitive primary and quaternary structures made it amenable to a genetic analysis using in-frame insertions and deletions. Length-altered proteins were characterized for the ability to perform the protein's three known functions: participation in particle assembly, genome translocation, and stimulation of viral protein synthesis. Insertion mutants were viable. Theoretically, these proteins would produce an assembled tube exceeding the capsid's internal diameter, suggesting that virions do not contain a fully assembled tube. Lengthened proteins were also used to test the biological significance of the crystal structure. Particles containing H proteins of two different lengths were significantly less infectious than both parents, indicating an inability to pilot DNA. Shortened H proteins were not fully functional. Although they could still stimulate viral protein synthesis, they either were not incorporated into virions or, if incorporated, failed to pilot the genome. Mutant proteins that failed to incorporate contained deletions within an 85-amino-acid segment, suggesting the existence of an incorporation domain. The revertants of shortened H protein mutants fell into two classes. The first class duplicated sequences neighboring the deletion, restoring wild-type length but not wild-type sequence. The second class suppressed an incorporation defect, allowing the use of the shortened protein.

IMPORTANCE

The H-tube crystal structure represents the first high-resolution structure of a virally encoded DNA-translocating conduit. It has similarities with other viral proteins through which DNA must travel, such as the α-helical barrel domains of P22 portal proteins and T7 proteins that form tail tube extensions during infection. Thus, the H protein serves as a paradigm for the assembly and function of long α-helical supramolecular structures and nanotubes. Highly repetitive in primary and quaternary structure, they are amenable to structure-function analyses using in-frame insertions and deletions as presented herein.

Bacteriophages have evolved several mechanisms to transport hydrophilic genomes through cell walls containing hydrophobic membranes and peptidoglycan. Myoviruses and podoviruses carry tails that, respectively, utilize contractile sheaths (1) and form extensions within the membrane (2). In contrast, siphoviruses, filamentous phage, and other tail-less viruses co-opt host cell membrane channels for penetration (3–5). However, the tail-less microvirus ϕX174 does not require a host-provided conduit for genome transport. Instead, genome translocation is mediated by 10 to 12 copies of the DNA-piloting protein H found inside the virion (6–8).

The X-ray structure of H protein's coiled-coil domain (8, 9) shows 10 parallel proteins oligomerized into a tube (Fig. 1) The tube is wide enough for passage of the single-stranded DNA (ssDNA) genome and has been visualized spanning the cell wall. It represents the first high-resolution structure of a virally encoded DNA-translocating conduit, sharing structural similarities with other viral proteins involved in DNA transport. For example, the H structure is entirely α-helical, similar to the α-helical barrel domain seen in the P22 portal protein (10, 11). Furthermore, it shares sequence similarities with T7 DNA-piloting proteins that form tail tube extensions during infection (2, 8). Thus, H protein serves as a paradigm for the assembly and function of long α-helical supramolecular structures and nanotubes (12, 13).

Protein H likely assumes multiple conformations during the ϕX174 life cycle. For DNA translocation, 10 proteins form a 170-Å-long α-helical tube that is separated into two domains. The N-terminal domain is composed of 3 11-amino-acid repeating units (hendecads), whereas the C-terminal domain is composed of 11 7-amino-acid units (heptads). Each repeating unit is directly aligned with the equivalent units of neighboring H proteins. Although an oligomer is required for DNA translocation, H proteins are monomeric in early assembly intermediates (14, 15). Tubes have not been visualized in procapsids or virions, but structure determination assumed icosahedral symmetry. Therefore, the timing and location of H-tube assembly have yet to be determined. The H-tube could exist as a fully assembled tube within the capsid or a partially assembled core, or it ϕmay only assemble externally at the infection site. Lastly, H protein likely assumes a third conformation, one required to stimulate viral protein synthesis (16).

Received 17 May 2016 **Accepted** 16 June 2016

Accepted manuscript posted online 29 June 2016

Citation Roznowski AP, Fane BA. 2016. Structure-function analysis of the ϕX174 DNA-piloting protein using length-altering mutations. J Virol 90:7956–7966. doi:10.1128/JVI.00914-16.

Editor: R. M. Sandri-Goldin, University of California, Irvine

Address correspondence to Bentley A. Fane, bfane@email.arizona.edu.

A

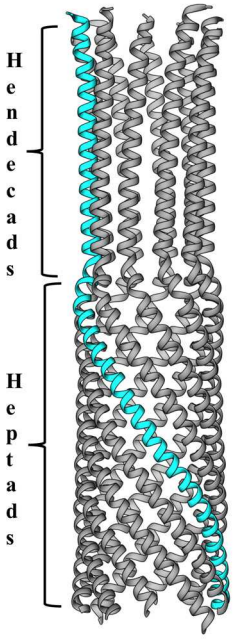

B

Wild-type primary structure

Position and sequence	Name
151 QKELTKMQLDN	Hendecad 1
162 QKEIAEMQNET	Hendecad 2
173 QKEIAGIQSAT	Hendecad 3
184 SRQNTKDQVYA	Transition
195 QNEMLAY	Heptad 1
202 QQKESTA	Heptad 2
209 RVASIME	Heptad 3
216 NTNLSKQ	Heptad 4
223 QQVSEIM	Heptad 5
230 RQMLTQA	Heptad 6
237 QTAGQYF	Heptad 7
244 TNDQIKE	Heptad 8
251 MTRKVSA	Heptad 9
258 EVDLVHQ	Heptad 10
265 QTQNQRY	Heptad 11

C H+14 sequence:

Heptad 10	Inserted heptads	Heptad 11
EVDLVHA	NTARTHV ETDRSKQ	QTQNQRY
	I H Y L	

Suppressors of *cs* phenotype

D H+11 Sequence:

Hendecad 1	Hendecad 2	Inserted Hendecad	Hendecad 3
QKELTKMQLDN	QKELAEMQNET	QKDLAEMQNET	QKDIAGIQSAT

E Δ11-1+11 sequence:

Duplicated hendecads		Hendecad 3
QKEIAEMQNET	QKEIAEMQNET	QKEIAGIQSAT

FIG 1 H protein structure and sequence. (A) Crystal structure of the H protein coiled-coil domain (PDB code 4JPP). A single monomer is shown in cyan. (B) Sequence of the H protein's structured region. Hendecad and heptad start positions, sequences, and numerical designations are listed. (C) Sequence and position of the 14 inserted amino acids found in the *H + 14* mutant. Mutant residues are underlined. Arrows indicate mutated residues found in *cs* revertants. (D) Sequence and position of the inserted hendecad found in the *H + 11* mutant. (E) Sequence and position of the hendecad duplication found in the *Δ11-1* revertant.

Taking advantage of the tube's repetitive structure, we conducted a genetic analysis: altering the protein's length by the addition or deletion of heptad and hendecad motifs. These mutations were used to determine whether larger H proteins could be accommodated within the volumetrically constrained capsid or if smaller H proteins could span the cell wall for DNA delivery. Length-altered proteins were also assayed for function during the intracellular stages of the ϕX174 life cycle: incorporation during assembly and the ability to stimulate the synthesis of other viral proteins.

MATERIALS AND METHODS

Phage plating, media, buffers, and stock preparation. Plating, media, buffers, and stock preparation have been previously described (17).

Bacterial strains, phage strains, and plasmids. The *Escherichia coli* C strains C 122 (Su^-), BAF5 (*supE*), and BAF30 (*recA*) have been previously described (17, 18). RY7211 contains a mutation in the *mraY* gene, conferring resistance to viral E protein-mediated lysis (19).

The ϕX174 H gene was cloned by PCR amplification. DNA between nucleotides 2931 and 3917 in the published sequence (20) was amplified with primers that introduced an XbaI site upstream of the gene's start codon and a downstream XhoI site. The PCR product was digested with XbaI and XhoI and ligated into pSE420 DNA (Invitrogen) digested with the same enzymes.

Cloned Δ11 H genes were constructed by first PCR amplifying the gene's 5′ region up to the hendecad to be deleted. The upstream primer introduced an XbaI site as described above. The introduced downstream restriction sites were SacII for the Δ11-1 gene, NaeI for the Δ11-2 gene, and SpeI for the Δ11-3 gene. The PCR product and pSE420 were digested with the desired enzymes and ligated. The remaining 3′ H gene codons were then PCR amplified with primers introducing restriction sites at each end of the product. The downstream primer introduced an XhoI site, while the upstream primers introduced the matching restriction site downstream of the 5′ cloned fragment. The PCR products and the respective cloned 5′ genes were digested and ligated.

Clones of all Δ7 and Δ14 H genes were constructed by directly mutagenizing the cloned ϕX174 H gene. Primers were designed to flank the heptad(s) to be deleted. The entire plasmid was then PCR amplified using Q5 DNA polymerase (New England BioLabs [NEB]) and the requisite primers. The PCR product's 5′ hydroxyl termini were phosphorylated and ends ligated using T4 polynucleotide kinase and ligase (New England BioLabs), respectively. The nucleotide sequence of all clones was verified by a direct DNA sequencing analysis.

The H + 14 clone was generated by first PCR amplifying nucleotides 2931 to 3719 of the ϕX174 sequence, which includes the 5′ region of gene H up to the insertion site for the additional 14 codons. The upstream primer introduced an XbaI site as described above. The downstream primer introduced seven codons of the inserted sequence and a BmgBI restriction site. The PCR product was digested with XbaI and BmgBI and ligated into pSE420 digested with the same enzymes. ϕX174 nucleotides 3720 to 3917 were then PCR amplified. The upstream primer introduced a BmgBI restriction site along with the remaining seven codons of the inserted sequence. The downstream primer introduced an XhoI site. The PCR product and the previously constructed clone were digested with BmgBI and XhoI. The digestion products were ligated, resulting in the cloned H + 14 gene.

ϕX174 *H + 14* was generated via recombination-rescue with a non-expressing H + 14 clone. A mutant containing an amber mutation at codon E265 in gene H, the *am*(*H*)*E265* mutant, was plated on cells containing the plasmid at 37°C. Plaques that developed at a frequency higher than the am^+ reversion frequency were isolated. The H genes were sequenced to confirm the presence of the inserted codons.

To generate the ϕX174 *Δ11-1am* and *Δ11-2am* amber mutants, ssDNA was first mutated by site-directed mutagenesis as previously described (21). For the *Δ11-1am* mutant, Eco53KI and EcoRV restriction sites were, respectively, introduced into gene H codons 154 and 165 and 166 along with an amber mutation in codon 151. For the *Δ11-2am* mutant, Eco53KI and EcoRV restriction sites were, respectively, introduced in codons 164 and 165 and 175 and 176 with an amber mutation in codon 158. The mutated DNA was transfected into cells expressing the wild-type H gene. The resulting amber mutants were isolated and their replicative-form (RF) DNA was purified as previously described (22), digested with the requisite enzymes, and religated. The ligation product was transfected into cells expressing the H gene of phage α3, and the resulting *Δ11-1am* and *Δ11-2am* mutants were isolated and sequenced to verify the genotype.

The ϕX174 *Δ7-3*, *Δ7-10am*, *Δ11-3*, *Δ14-2&3*, *Δ14-3&4*, *Δ14-9&10*,

and Δ*14-10*&*11am* mutants were generated using the same method as used to generate Δ7 and Δ14 H gene clones. Primers flanked the hendecad or heptad(s) to be deleted and, if necessary, introduced amber codons. The entire genome was then PCR amplified with Q5 DNA polymerase (NEB) and the described primers. The product's 5′ hydroxyl termini were phosphorylated and ends ligated using T4 polynucleotide kinase and ligase (NEB), respectively. The resulting viral genomes were transfected into cells expressing the H gene of phage α3. Mutants were isolated as described above and sequenced to verify their genotypes.

Generation of ssDNA and double-stranded RF DNA, rate zonal sedimentation, and protein electrophoresis. The protocols for ssDNA and double-stranded RF DNA isolation and purification, rate zonal sedimentation, and protein electrophoresis protocols have been previously described (21–23).

Attachment, eclipse, and coat protein quantification. Attachment and eclipse assays have been previously described (24, 25). Coat protein quantification as a surrogate marker for genome piloting was performed as follows. Phage were preattached to RY7211 cells infected at a multiplicity of infection (MOI) of 1.0 in HFB buffer (17) at 15°C and incubated for 30 min. The infected cells were pelleted at 4°C and the supernatant was removed. Infected cells were suspended in 1.0 ml of iced TKY medium (1.0% tryptone, 0.5% KCl, 0.5% yeast extract) with 10 mM $MgCl_2$ and 5.0 mM $CaCl_2$. The infected cells were added to 9.0 ml of TKY broth with 10 mM $MgCl_2$ and 5 mM $CaCl_2$ warmed to the experimental temperatures. At the desired time points, 1.0-ml aliquots were pelleted and resuspended in 0.1 ml of HFB buffer. Ten microliters of the concentrated sample was diluted into 90 μl of BE buffer (17) containing 10 mg/ml of lysozyme. Infected cells were allowed to lyse overnight at 4°C, and the titers of released virions were determined. The remainder of the concentrated sample was placed at −20°C immediately after collection. Thirty-microliter volumes of the concentrated samples were run on SDS-PAGE gels as previously described (23). SDS-PAGE gels were stained with Coomassie brilliant blue and digitized with a LICOR scanner. Relative coat protein levels were determined by densitometry analysis using ImageJ software (NIH). Coat protein intensity was normalized to the intensity of a host protein band indicated in Fig. 3.

RESULTS

Tube length can be increased beyond the internal diameter of the capsid. Although the ϕX174 H-tube structure is a 170-Å-long decamer, H proteins are incorporated as monomers during assembly (14, 15). Thus, it is unknown whether they exist within the capsid as a fully formed tube, as a partially constructed core, or as monomers ready to complete assembly at the infection site. The related bacteriophage G4 encodes two extra heptad motifs within its coiled-coil domain, yet the G4 capsid has the same internal capsid diameter as ϕX174, 172 Å. The additional G4 heptads are predicted to assume a helical structure (26) If the prediction is correct, the additional heptads would lengthen the tube by ~18 Å. While this suggests that the tube is not fully assembled within the mature virion, the internal diameter of the G4 capsid was derived from a degraded procapsid, not a mature virion (26). To rigorously test whether a fully assembled tube exists in the capsid, DNA encoding the two additional G4 heptads was placed within the ϕX174 H gene (*H + 14*). If a fully assembled tube is not encapsidated, motif insertions should not inhibit tube assembly or genome piloting. In the structure, neighboring H proteins are bound together via specific interhelical contacts between identical heptad and hendecad motifs (Fig. 1A). If motif alignment is maintained, additional units should not dramatically disrupt contacts or reduce tube integrity. Alternatively, if viability requires the internal assembly of a complete tube, lengthened H proteins will result in noninfectious particles.

TABLE 1 Plating efficiencies of *H + 14* and revertants

Genotype of ϕX174	Plating efficiency[a] at:		
	24°C	33°C	42°C
Wild type	0.6	1.0	0.9
H + 14	1×10^{-4}	1.0	0.9
H + 14 T3I[b]	4×10^{-2}	1.0	1.5
H + 14 R5H	0.3	1.0	0.6
H + 14 H7Y	0.2	1.0	0.5
H + 14 R12L	0.1	1.0	0.5

[a] Plating efficiency is defined as assay titer/titer at 33°C.
[b] Revertant names reflect the amino acid substitution found within the inserted two heptads. Thus, T3I indicates a T→I substitution for amino acid 3 of the inserted sequence (Fig. 1C).

The resulting *H + 14* mutant was viable but exhibited a cold-sensitive (*cs*) phenotype at 24°C. This defect was rescued by a variety of point mutations within the inserted codons (Table 1; Fig. 1C). To determine if the mutant virions were as infectious as wild-type virions, permissively synthesized *H + 14* particles as well as a *cs* revertant (*H + 14 R12L*) were purified by rate zonal sedimentation and their specific infectivity (PFU/A_{280}) was determined. As can be seen in Fig. 2A, both mutant viruses sediment like the wild type: the A_{280} peak coincides with the specific infectivity peak at 114S. The protein composition was analyzed by SDS-PAGE (Fig. 2C). Elongated proteins were observed in mutant particles at wild-type levels as determined by densitometry (data not shown). The specific infectivity of the *H + 14* mutant was reduced compared to that of the wild type (Fig. 2B). However, reversion of the *cs* phenotype (*H + 14 R12L*) restored specific infectivity to wild-type levels. The *H + 14 R12L* mutant's wild-type phenotype suggests that elongated proteins can be fully tolerated. Thus, it is unlikely that virions contain a fully assembled H-tube. Similar results were obtained with the *H + 11* mutant, which contains a duplication of a ϕX174 hendecad (Fig. 1D; see also below). Unlike the aforementioned G4-derived heptads, this hendecad is known to form a straight helix in the X-ray structure (8).

The ϕX174 *H + 14 cs* phenotype reflects a kinetic assembly defect. H protein is involved in multiple aspects of the viral life cycle, from host attachment to intracellular assembly. Previously characterized mutants exhibited both attachment and assembly defects (27, 28). Therefore, all aspects of the ϕX174 *H + 14* life cycle were analyzed. In both attachment and eclipse assays conducted at 24°C, the mutant performed like the wild type (data not shown). Thus, the kinetics of attachment and the initiation of DNA transport (eclipse) did not appear to be affected.

Eclipse assays detect the loss of infectivity, which occurs at the initiation of DNA piloting. However, they do not determine whether DNA was transported into the cytoplasm. Mutations could prevent tube assembly, stall DNA mid-transit, or lower tube integrity but not affect eclipse kinetics. In a wild-type infection, a portion of the (+) ssDNA genome enters the cytoplasm. Host polymerases then complete genome translocation by synthesizing the complementary (−) strand (29), a prerequisite to viral transcription and translation. Thus, the kinetics of coat protein synthesis can serve as a surrogate marker for genome piloting. Lysis-resistant cells were infected at 24°C with wild-type ϕX174 or the *H + 14* or *H + 14 R12L* mutant. At designated time points, aliquots were removed and whole-cell lysates analyzed by SDS-PAGE (Fig. 3A). Coat protein band intensity was quantified rela-

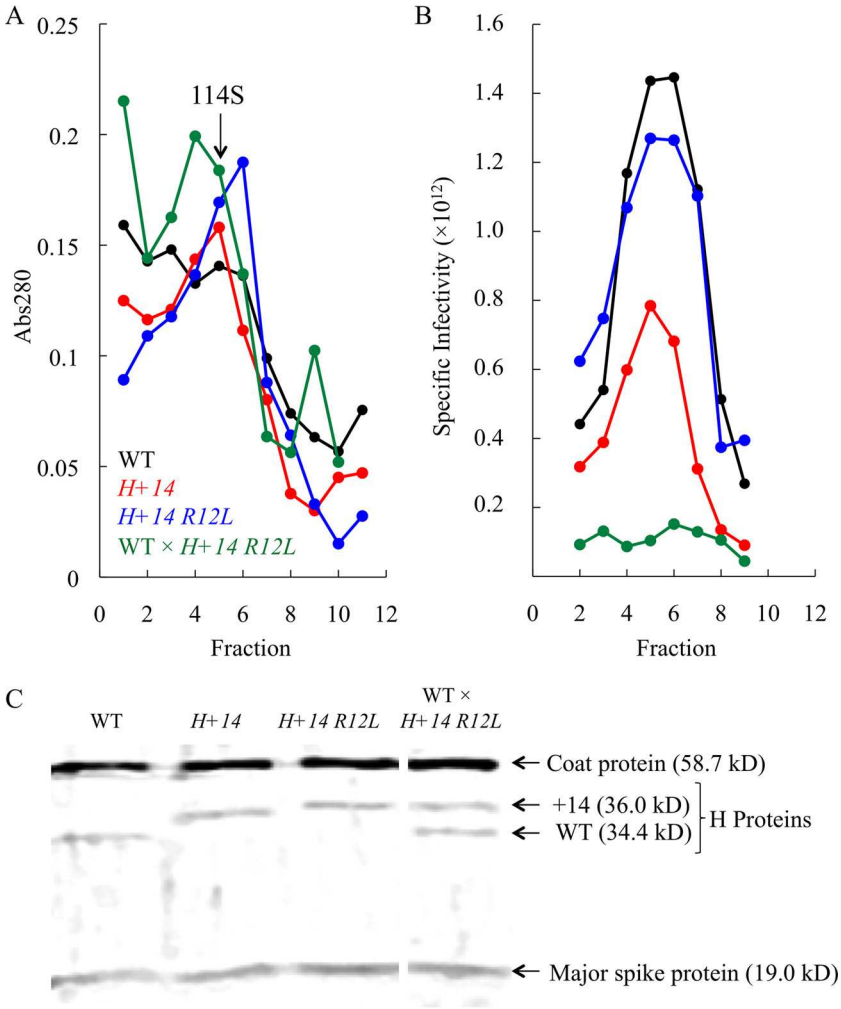

FIG 2 Assembled particles produced in cells infected with the wild type (black) and *H + 14* (red), and *H + 14 R12L* (blue), and wild-type × *H + 14 R12L* (green) mutants. (A) A_{280} profiles of infected-cell extracts analyzed by rate zonal sedimentation. Fraction 1 represents the gradient bottom. The fraction was the highest specific infectivity is indicated with an arrow and marked 114S. (B) Specific infectivity (PFU/A_{280}) of fractions. (C) SDS-PAGE analysis of 114S peaks. The white space between lanes 3 and 4 indicates the removal of irrelevant bands from the gel.

tive to a host protein band (Fig. 3B). The appearance and accumulation of coat protein in *H + 14* mutant-infected cells closely matched those in cells infected with the wild type, suggesting that genome piloting is not dramatically affected at the restrictive temperature.

During the same experiment, the kinetics of virion production were also monitored; at each time point, samples of infected cells were chemically lysed, and titers of infectious particles were determined. The kinetics of *H + 14* progeny production were significantly reduced (Fig. 3C). Wild-type titers exceeded the input value at 100 min postinfection, whereas *H + 14* mutant titers did not reach that level until 150 min postinfection. Slow assembly likely prevents *H + 14* mutant plaque formation on lysis-sensitive cells. Lysis is programmed to occur during host division (30). Progeny must be produced prior to this event, which occurred at approximately 110 min during these experiments. The R→L substitution in the *H + 14 R12L cs* revertant partially alleviated this kinetic defect. However, kinetics were not restored to wild-type levels (see Discussion).

The reduced infectivity of virions containing two species of piloting protein further validate the X-ray structure. In the H-tube, monomers are bound together through a set of specific interhelical contacts. As seen in other coiled-coil structures (31), these contacts keep monomers parallel and in register, aligning equivalent heptad and hendecad motifs. This arrangement likely confers stability during tube assembly and/or DNA piloting. A virion containing H proteins of differing lengths could not achieve this arrangement and may not assemble into a functional tube. Since H proteins are incorporated as monomers during assembly, it is possible to assemble particles containing a heterogeneous complement of H proteins. However, these particles should exhibit reduced infectivity. To test this hypothesis, lysis-resistant cells were coinfected with the wild type and the equally infectious *H + 14 R12L* mutant at 37°C. Particles were purified and assayed for protein content and specific infectivity. As shown in Fig. 2C, the wild-type and *H + 14 R12L* H proteins were found in particles at approximately equal levels. The specific infectivity of the heterogeneous particles was reduced compared to those of homogeneous wild-type and *H + 14 R12L* populations (Fig. 2B). Similar results were obtained for wild-type-infected cells expressing the cloned *H + 14 R12L* gene (data not shown).

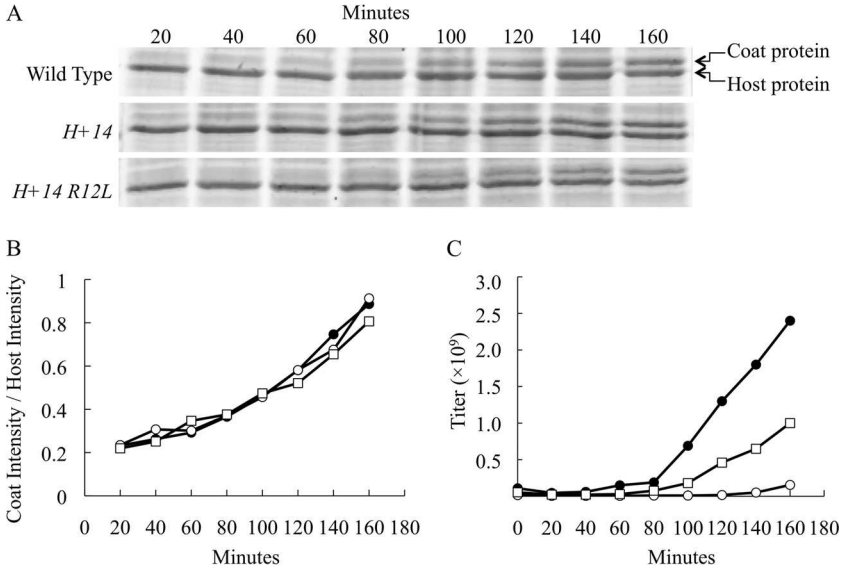

FIG 3 Characterization of the *H + 14* mutant. (A) SDS-PAGE analysis of cells infected with either the wild type or the *H + 14* or *H + 14 R12L* mutant. (B) Quantification of coat/host protein ratios seen in panel A. Black circles, wild type; white circles, *H + 14* mutant; white squares, *H + 14 R12L* mutant. The host protein used in this analysis is indicated in panel A. (C) Titers of progeny produced in cells infected with the wild type (black circles), *H + 14* mutant (white circles), or *H + 14 R12L* mutant (white squares).

Proteins with deleted hendecad and heptad motifs fail to transport DNA or are not incorporated into virions. During genome piloting, the coiled-coil domain spans the periplasmic space or a membrane adhesion zone (8, 32). A minimal length is likely required to bridge this gap. Although characterizing the phenotypes associated with length-shortened tubes could directly address this question, internal deletions could also affect H protein incorporation or oligomerization. To explore these possibilities, nine cloned H genes with internal deletions were constructed. The mutant genes lacked DNA encoding a single hendecad (Δ11), a single heptad (Δ7), or two sequential heptads (Δ14). Cloned-gene expression was assayed for the ability to complement an *am*(*H*) mutant or inhibit wild-type plaque formation. Unlike the cloned wild-type gene, the mutant genes were unable to complement (Table 2). Although wild-type plating efficiency was not significantly lowered, the expression of the Δ11-1 and Δ11-2 genes reduced wild-type plaque size. Expression of the remaining genes, the Δ11-3, Δ7-3, Δ7-10, Δ14-2&3, Δ14-3&4, Δ14-9&10, and Δ14-10&11 genes, did not affect wild-type plating efficiency or plaque size.

To determine whether the ΔH proteins failed to function in DNA transport or were not incorporated during assembly, lysis-resistant cells expressing the deletion constructs were infected with an *am*(*H*) mutant. The resulting particles were purified (Fig. 4A and B), and their protein composition (Fig. 4D and E) and specific infectivity (Table 3) were determined. In this assay, specific infectivity is strictly defined as PFU/A_{280}, regardless of the genotype of the plaque-forming particle. For particles generated in cells expressing the mutant H genes, plaques were formed by am^+ revertants. Thus, the actual specific infectivity of the mutant particles is lower than the assay suggested.

The sedimentation profiles of the *am*(*H*) infections are depicted in Fig. 4A and B. Particles containing mutant H proteins or lacking H protein are known to sediment at 110S and/or 70S (33). Therefore, naturally occurring am^+ revertants were used to estimate particle S values. When the *am*(*H*) mutant was complemented by the cloned wild-type gene, particle infectivity and absorbance peaks aligned. In contrast, particles from infections with uncomplemented mutants or from cells expressing the Δ7 and Δ14 H genes migrated in two distinct peaks. The material in the faster peak migrated slightly slower than 114S. As previously documented for particles that sediment at 110S (33), these particles exhibited a reduced specific infectivity (Table 3) and lacked scaffolding proteins (Fig. 4D and E). The A_{260}/A_{280} ratios, used to estimate DNA content, did not significantly differ from that of the wild type (data not shown). The rightmost peak is likely composed

TABLE 2 Wild-type and *am*(*H*) mutant plating efficiencies in cells expressing Δ7, Δ11, or Δ14 H genes at 33°C

Expressed gene	Plating efficiency[a] of:		Wild-type[c] plaque size reduction of >50%
	am(*H*) mutant[b]	Wild type	
None	6.0×10^{-5}	1.0	No
Wild-type H	1.0	1.1	No
Δ7-3	1.5×10^{-4}	1.1	No
Δ7-10	1.6×10^{-4}	1.0	No
Δ14-2&3	1.6×10^{-4}	1.1	No
Δ14-3&4	1.8×10^{-4}	1.1	No
Δ14-9&10	1.7×10^{-4}	0.8	No
Δ14-10&11	1.9×10^{-4}	0.9	No
Δ11-1	$<4.0 \times 10^{-6}$	0.5	Yes
Δ11-2	2.0×10^{-4}	1.2	Yes
Δ11-3	2.0×10^{-4}	1.5	No

[a] For the *am*(*H*) mutant, plating efficiency is defined as assay titer/titer on cells expressing the wild-type H gene. For the wild type, it is defined as assay titer/titer on cells with no cloned gene expression.
[b] The *am*(*H*)*G7* mutant was used in the experiments with Δ7 and Δ14 H genes, whereas the *am*(*H*)*Q158* mutant was used in experiments with Δ11 genes. The two amber mutants exhibited the same am^+ reversion frequency.
[c] Plaques were compared to those formed on cells expressing the wild-type H gene.

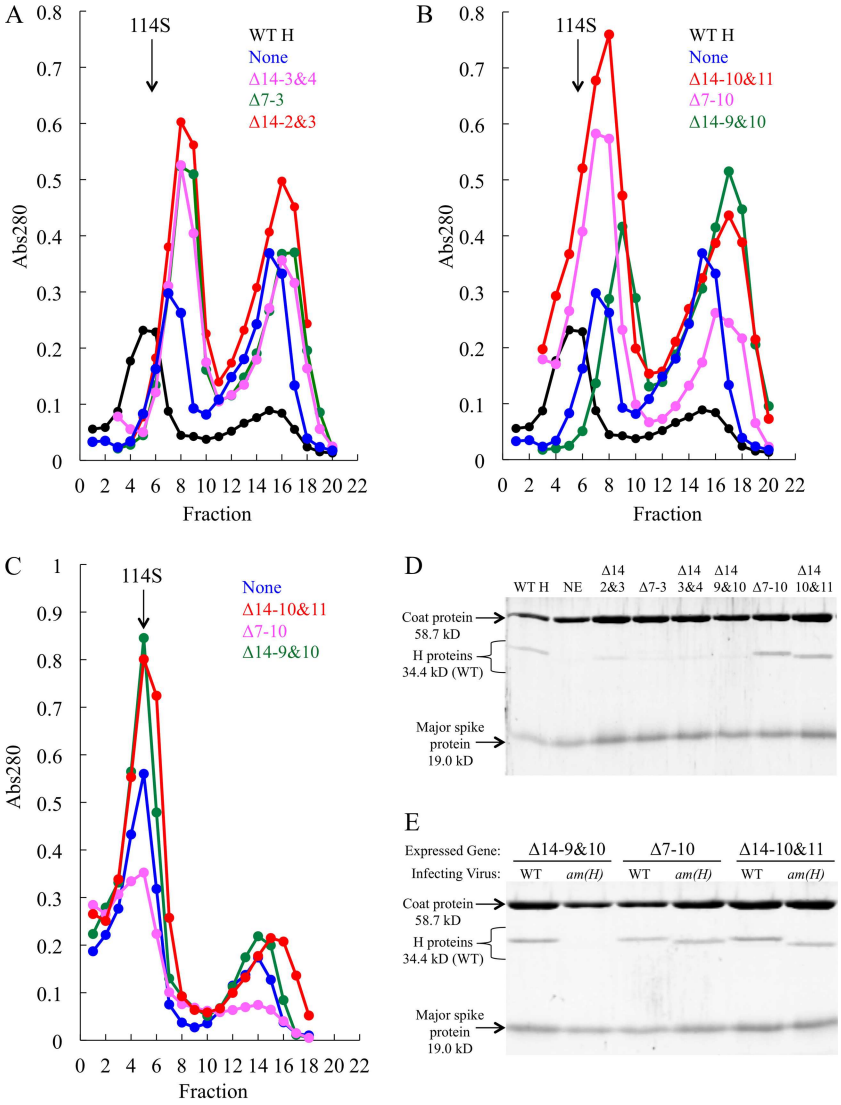

FIG 4 Characterization of the Δ7 and Δ14 proteins in *am*(*H*) mutant- or wild-type-infected cells. A_{280} absorbance profiles of extracts of cells infected with either *am*(*H*) (A and B) or the wild type (C), analyzed by rate zonal sedimentation. Particles were assembled in cells expressing cloned wild-type H and various ΔH genes as indicated. Fraction 1 represents the gradient bottom. The fraction with the highest specific infectivity is indicated with an arrow and marked 114S. (D) SDS-PAGE analysis of particles produced in *am*(*H*) mutant-infected cells expressing cloned wild-type H (WT H), Δ7-3, Δ7-10, Δ14-2&3, Δ14-3&4, Δ14-9&10, and Δ14-10&1 genes or nonexpressing cells (NE). (E) SDS-PAGE analysis comparing wild-type and *am*(*H*) particles synthesized in cells expressing the Δ7-10, Δ14-9&10, or Δ14-10&11 gene.

of 70S particles. Noninfectious, they arise from aborted genome packaging attempts or premature eclipse (33).

Although all infections of Δ7- and Δ14 gene-expressing cells produced assembled particles (Fig. 4A and B), H protein content varied depending on which heptad(s) was deleted (Fig. 4D). Only the proteins lacking just the 10th or both the 10th and 11th heptads appeared to be incorporated efficiently. However, the expression of these cloned genes did not affect wild-type plating efficiency or plaque size, as would be expected if virions contained H proteins of two different lengths. This suggests that the shortened proteins cannot compete with the wild-type protein for incorporation. To test this hypothesis, cells expressing the cloned Δ7-10 or Δ14-10&11 genes were infected with either wild-type or *am*(*H*) ϕX174. Cells expressing the cloned Δ14-9&10 gene were used as a control for an unincorporated protein. Expression of the cloned genes did not appear to affect wild-type progeny sedimentation (Fig. 4D): infectivity and A_{280} peaks coincided, and specific infectivity was not significantly reduced (Table 3). Particles were analyzed by SDS-PAGE (Fig. 4E). For each exogenously expressed ΔH gene, the particles synthesized in cells infected with either the wild type or the *am*(*H*) mutant were analyzed adjacent to each other. The wild-type H protein migrates more slowly than the ΔH proteins. While the Δ7-10 or Δ14-10&11 proteins are present in the particles produced in the *am*(*H*) mutant infections, only the larger wild-type protein is present in the particles isolated from wild-type-infected cells.

A similar analysis was conducted with Δ11 proteins. *am*(*H*) progeny produced in cells expressing Δ11 H genes were characterized as described above. The resulting particles were not infectious and migrated slower than 114S (Fig. 5A and Table 3). H protein

TABLE 3 Specific infectivities of 110S-114S particles produced in *am*(*H*)*G7* and wild-type infections in cells expressing Δ7, Δ11, or Δ14 genes

Virus	Expressed gene	Specific infectivity (PFU/A_{280})[a]		H proteins incorporated[d]	Corresponding figure
		Raw[b]	Normalized[c]		
am(*H*)G7 mutant	None	2.0×10^{10}	2.0×10^{-2}	None	4A, B, and D
	WT H	9.0×10^{11}	1.0	Yes	4A, B, and D
	Δ7-3	9.0×10^{9}	1.0×10^{-2}	None	4A and D
	Δ7-10	4.0×10^{9}	5.0×10^{-3}	Yes	4B, D, and E
	Δ14-2&3	7.0×10^{9}	8.0×10^{-3}	Trace	4A and D
	Δ14-3&4	2.0×10^{10}	2.0×10^{-2}	Trace	4A and D
	Δ14-9&10	2.0×10^{8}	2.0×10^{-4}	No	4B, D, and E
	Δ14-10&11	2.0×10^{8}	2.0×10^{-4}	Yes	4B, D, and E
Wild type	None	2.0×10^{12}	1.0	WT	4C and E
	Δ7-3	9.0×10^{11}	0.5	Only WT	Data not shown
	Δ7-10	2.0×10^{12}	0.8	Only WT	4C and E
	Δ14-2&3	1.0×10^{12}	0.6	Only WT	Data not shown
	Δ14-3&4	2.0×10^{12}	1.1	Only WT	Data not shown
	Δ14-9&10	2.0×10^{12}	1.2	Only WT	4C and E
	Δ14-10&11	1.0×10^{12}	0.8	Only WT	
am(*H*)*G7*	WT H	4.0×10^{11}	1.0	Yes	5A and C
	Δ11-1	2.0×10^{8}	5.0×10^{-4}	Yes	5A and C
	Δ11-2	2.0×10^{8}	5.0×10^{-4}	Yes	5A and C
	Δ11-3	4.0×10^{7}	9.0×10^{-5}	No	5A and C
Wild type	None	4.0×10^{11}	1.0	WT	5B and C
	Δ11-1	2.0×10^{10}	7.0×10^{-2}	Both proteins	5B and C
	Δ11-2	2.0×10^{10}	4.0×10^{-2}	Both proteins	5B and C
	Δ11-3	4.0×10^{11}	1.1	Only WT	5B and C

[a] In these assays specific infectivity is strictly defined as PFU/A_{280}, regardless of the genotype of the plaque-forming particle (see the text for details).
[b] Raw data are PFU/A_{280}.
[c] For experiments conducted with *am*(*H*)*G7*, data are normalized to the specific infectivity of particles generated in cells expressing the wild-type H gene. For experiments conducted with wild-type ϕX174, data are normalized to the specific infectivity of particles generated in cells without mutant cloned-gene expression.
[d] For experiments conducted with the *am*(*H*)*G7* mutant, "Yes" indicates that mutant H protein was found at levels comparable to the particles generated in cells expressing the wild-type H gene, "No" indicates that H protein levels were below the sensitivity required for detection, and "Trace" indicates that a faint amount of protein could be detected by SDS-PAGE.

content varied depending on which hendecad motif was deleted. As can be seen in Fig. 5C, Δ11-1 and Δ11-2 proteins were incorporated into particles, whereas Δ11-3 proteins were not. As previously described, Δ11-1 and Δ11-2 gene expression reduced wild-type plaque size. To investigate this dominant negative effect, cells expressing Δ11 constructs were infected with the wild-type virus (Fig. 5B). Particles synthesized in Δ11-1 and Δ11-2 gene-expressing cells exhibited a reduced infectivity compared to those assembled in Δ11-3 gene-expressing or -nonexpressing cells (Table 3). The Δ11-1 and Δ11-2 proteins were incorporated at approximately equal levels alongside the wild-type protein (Fig. 5C). Incorporation of the Δ11-1 and Δ11-2 proteins likely reduced both infectivity and plaque size.

Irrespective of functional piloting and incorporation, all mutant proteins retain some level of function. In addition to the aforementioned functions, *de novo* H protein synthesis is required for the efficient production of other viral proteins (16). To determine if the Δ7, Δ11, and Δ14 H proteins retained the last function, lysis-resistant cells expressing the ΔH gene constructs were infected with an *am*(*H*) mutant. The resulting whole-cell lysates were examined by SDS-PAGE 3 h postinfection. Without complementation, the amount of viral coat protein seen in lysates of cells infected with the *am*(*H*) mutant is greatly diminished (Fig. 6, top, rightmost lane). Complementation with the wild type or any of the ΔH genes restored coat protein levels to that observed in infections with the wild type. This result demonstrates that once in the cell, this additional function occurs independently of the protein's ability to be incorporated into particles.

Reversion analysis of ΔH mutants. To determine if the virus could adapt and utilize the ΔH proteins, a reversion analysis was conducted. For this analysis, the ΔH genes were constructed directly within the ϕX174 genome instead of being expressed from a plasmid. This allows selective pressure to be applied to all viral genes. The resulting strains displayed a complementation-dependent phenotype, growing only in cells expressing a cloned wild-type gene (Table 4). A cloned H gene from the related α3 bacteriophage also complemented. Based on sequence similarities, the overall architecture and length of the α3 and ϕX174 coiled-coil domains are identical. To avoid recovering wild-type recombinants when selecting for second-site revertants, ΔH mutants were propagated in cells expressing the α3 H gene before the selection. Although the Δ*7-10*, Δ*11-1*, Δ*11-2*, and Δ*14-10&11* mutants were recovered, they could not be propagated in cells synthesizing the α3 H protein, likely because the proteins could outcompete α3 H for incorporation. To alleviate this problem, an amber mutation was placed at a glutamine codon immediately upstream of the deleted hendecad or heptad(s), resulting in the Δ*7-10am*, Δ*11-1am*, Δ*11-2am*, and Δ*14-10*&*11am* mutants. Although this pre-

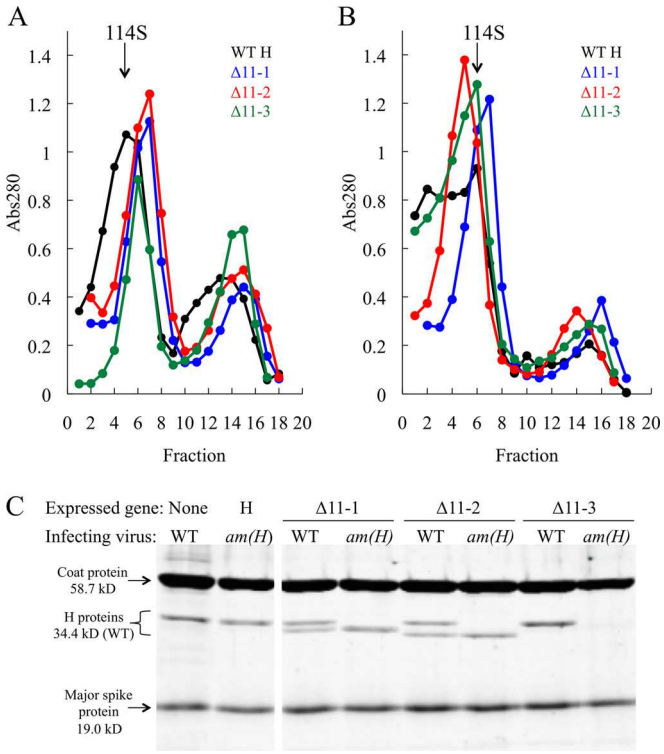

FIG 5 Characterization of the Δ11 proteins in cells infected with the *am*(*H*) mutant or the wild type. A_{280} profiles of extracts of cells infected with either the *am*(*H*) mutant (A) or the wild type (B) were analyzed by rate zonal sedimentation. Particles were assembled in cells expressing cloned wild-type H and various ΔH genes as indicated. (C) SDS-PAGE analysis comparing wild-type (WT) and *am*(*H*) particles synthesized in cells expressing the Δ11-1, Δ11-2, or Δ11-3 H gene. The white space between lanes 2 and 3 indicates the removal of irrelevant bands from the gel.

vented the synthesis of the ΔH proteins during viral propagation, ΔH-utilizing mutants could still be isolated on *supE* cells. The *supE* informational suppressor inserts glutamine at amber codons during translation.

Revertants were selected for the loss of the complementation-dependent phenotype. Only two types of revertants were isolated, one each from the Δ*11-1am* and Δ*7-3* mutants. In the Δ*11-1am* revertant, the hendecad immediately following the deletion was duplicated. Thus, the revertant (Δ*11-1am* + *11*) possessed a wild-type number of hendecads but not a wild-type sequence. This mutant was independently isolated from two stocks; in each instance, it appeared at a frequency of 10^{-9}. Amber reversion resulted in the Δ*11-1* + *11* strain (Fig. 1E), which displayed a wild-type plating phenotype and specific infectivity (data not shown).

In addition, a more complex reversion event occurred during strain construction. The resulting *H* + *11* mutant contained four hendecads (Fig. 1D). Its phenotype and specific infectivity were similar to those of the wild type. In coinfections, both the wild-type and *H* + *11* proteins were incorporated into particles. These particles also exhibited a reduced specific infectivity, 4.7×10^{11} PFU/A_{280}, compared to 1.7×10^{12} PFU/A_{280} and 9.7×10^{11} PFU/A_{280} for the wild-type and *H* + *11* parents, respectively.

The Δ*7-3* revertant contained a true deletion utilizer. It was isolated from two independently grown stocks at a frequency of 10^{-8} (Table 4). A single point mutation in gene H, causing a G→V substitution at amino acid 80, restored plaque formation. Although utilizers of the other ΔH proteins were not found above a frequency of 10^{-9}, recombination rescue experiments were performed to determine if the G80V mutation was active in other backgrounds. Two plasmids containing only a portion of the H gene were used in these experiments. One plasmid contained the G80V mutation, while the other contained only wild-type sequence. As these plasmids contain only the first 149 codons of the complete 328 codon gene, Δ*H* or *am*(*H*) mutant plaque formation requires recombination with the plasmid. These results are presented in Table 4. A mutant with an amber mutation at codon 26, the *am*(*H*)*Q26* mutant, served as a positive control. In the absence of a complementing clone, it exhibited a reversion frequency of 4×10^{-6}. However, in the presence of the wild-type or G80V H gene fragments, plating efficiency rose to 10^{-3} and 9.0×10^{-4}, respectively. The higher plating efficiency on noncomplementing cells resulted from recombination rescue. The Δ*7-3* revertant produced viable recombinants in cells containing the G80V gene H fragment at a frequency of 3×10^{-4}. No viable recombinants were obtained in cells containing the wild-type gene H fragment (frequency $< 5.0 \times 10^{-7}$). The plating efficiencies of the remaining mutants—the Δ*7-10am*, Δ*11-1am*, Δ*11-2am*, Δ*11-3*, Δ*14-2*&*3*, Δ*14-3*&*4*, Δ*14-9*&*10*, and Δ*14-10*&*11am* mutants—were several orders of magnitude lower than the positive control, indicating that the G80V mutation is not active in these backgrounds.

DISCUSSION

Fully assembled tubes are unlikely to exist in the capsid. The inner diameter of the ϕX174 capsid is 172 Å, whereas the H-tube is 170 Å in length. The similar dimensions suggest that the assembled tube is not stored in the capsid. To test this hypothesis, tubes were theoretically lengthened by inserting either one hendecad or two heptad motifs, increasing the tube length by 16 or 18 Å, respectively. However, the X-ray structures of the length-altered proteins were not determined.

The *H* + *14* mutant displayed a *cs* phenotype and a reduced specific infectivity, approximately one-half the wild-type value. At

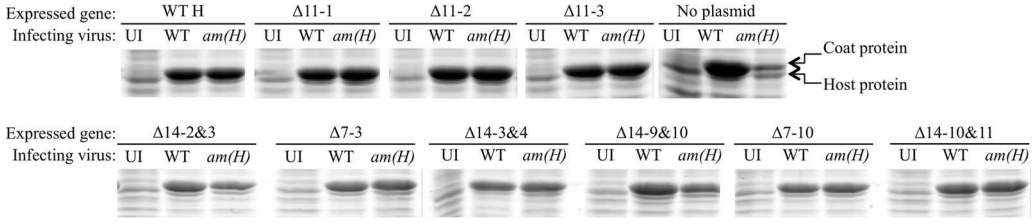

FIG 6 Viral protein levels in *am*(*H*) mutant-infected cells with and without ΔH gene expression. Viral coat protein levels in uninfected (UI), wild-type-infected (WT), and *am*(*H*) mutant-infected cells expressing the ΔH gene constructs.

TABLE 4 Plating efficiency and recombination rescue of Δ7, Δ11, and Δ14 mutant phage

Mutant	Plating efficiency and recombination rescue[a]			
	Expressed cloned gene		Unexpressed clone of codons 1-149	
	None	Wild-type H	Without G80V	With G80V
am(H)Q26	4.0×10^{-6}	1.0	**1.0×10^{-3}**	**9.0×10^{-4}**
Δ*11-1am*[b]	1.0×10^{-9}	1.0	$<3 \times 10^{-6}$	$<3 \times 10^{-6}$
Δ*11-2am*	$<3.0 \times 10^{-9}$	1.0	$<5 \times 10^{-7}$	$<5 \times 10^{-7}$
Δ*11-3*	$<2.0 \times 10^{-9}$	1.0	$<1.0 \times 10^{-6}$	$<1.0 \times 10^{-6}$
Δ*7-3*	$1.0 \times 1\ 0^{-8}$	1.0	$<5.0 \times 10^{-7}$	**3.0×10^{-4}**
Δ*7-10 am*	$<8.0 \times 10^{-9}$	1.0	$<1.0 \times 10^{-6}$	$<1.0 \times 10^{-6}$
Δ*14-2&3*	$<8.0 \times 10^{-10}$	1.0	$<8.0 \times 10^{-6}$	$<8.0 \times 10^{-6}$
Δ*14-3&4*	$<3.0 \times 10^{-10}$	1.0	$<2.0 \times 10^{-7}$	$<2.0 \times 10^{-7}$
Δ*14-9&10*	$<6.0 \times 10^{-10}$	1.0	$<3.0 \times 10^{-7}$	$<3.0 \times 10^{-7}$
Δ*14-10&11am*	$<1 \times 10^{-9}$	1.0	$<1 \times 10^{-6}$	$<1 \times 10^{-6}$

[a] Plating efficiency is defined as assay titer/titer on cells expressing the wild-type H gene. Bold text indicates recombination rescue.
[b] Plating efficiencies of deletion mutants containing amber mutations were calculated with titers obtained on *supE* cells containing the specified clone.

the restrictive temperature, attachment, eclipse, and DNA piloting appeared to be unaffected; however, mutant particles assembled more slowly than the wild-type control. The underlying molecular defect remains to be determined. The mutant H protein could be incorporated into pentameric assembly intermediates more slowly than the wild-type protein, or the resulting intermediates may be less efficiently organized into procapsids. Nonetheless, a single substitution within the inserted sequence (*H + 14 R12L*) suppressed the assembly defect and restored specific infectivity to the wild-type level. The nearly wild-type phenotype of the *H + 14 R12L*, as well as the wild-type phenotype of the *H + 11* mutant, demonstrates that the virus can tolerate these insertions. This result, along with the absence of an external tail-like structure, strongly suggests that the H-tube is not fully assembled in the capsid. The proteins may remain monomeric or could associate into a semiassembled, core-like structure. A core could be located in the virion's center or situated under a single 5-fold axis of symmetry, creating a unique vertex. Further structural studies are necessary to investigate these possibilities. Previous X-ray structures or electron microscopy (EM) reconstructions could not determine the location of H proteins due to the imposition of icosahedral averaging and/or noise created by the packaged DNA (8, 34, 35).

Defective particles containing functional H proteins of differing lengths support the biological significance of the X-ray structure. In the H-tube structure, equivalent heptad and hendecad motifs are aligned via specific interhelical contacts. This arrangement likely keeps the parallel α-helices in register, possibly guiding tube assembly and ensuring stability during genome piloting. If functional H proteins of differing lengths were packaged into the same particle, the length mismatch would place α-helices out of register and likely prevent proper tube assembly. To test the biological significance of this arrangement, cells were coinfected with wild-type and the equally infectious *H + 14 R→L* or *H + 11* mutants. The two H proteins were found at equal levels in the resulting 114S particle population, but a significant portion of the population was defective. The incorporation of both H protein species likely explains the loss of specific infectivity. This reduction was not complete; approximately 10% of particles were still infectious. Virions can carry 12 H proteins. However, only 10 compose an H-tube. Although some virions may contain 10 identical H proteins, the probability of this randomly occurring is far lower than 10% if each species of H protein is incorporated with equal efficiency. Indeed, the elongated and wild-type H proteins appear to be present in the progeny population at roughly equal levels. This suggests that a functional tube can be constructed with some heterogeneous protein combinations or that there is a *cis*-acting mechanism that partially governs assembly: i.e., virions are preferentially assembled from proteins translated from the same message. Similar results were obtained with the Δ11-1 and Δ11-2 deletion proteins that could effectively compete with the wild-type protein.

Deletions of hendecad and heptad motifs result in H protein incorporation defects and/or infectivity loss. The ΔH proteins can be divided into two groups: those that were incorporated into virions and those that were not. H proteins containing deletions within an 85-amino-acid segment, spanning the third hendecad to the ninth heptad, were not efficiently incorporated into particles (Fig. 4D). This region either contains an incorporation domain or is essential for its proper folding. However, a single amino acid substitution, G80V, in *cis* with the Δ*7-3* mutation resulted in viable virions. This suppressor is allele specific, rescuing only the Δ*7-3* mutant. This mutation resides 128 residues away from the deletion, possibly indicating that multiple regions affect incorporation. Alternatively, the G80V substitution may suppress competing off-pathway reactions favored by the Δ7-3 H protein. The other deletions may more efficiently promote these competing reactions, requiring multiple or stronger suppressors. Alternatively, the G80V substitution could rescue the incorporation of these proteins, but unlike Δ7-3 protein, they may be unable to form functional tubes. Our assays were based on the formation of viable progeny; thus, they do not distinguish between these models.

Proteins with deletions of the first two hendecads or the last two heptads were incorporated. However, these particles were uninfectious, indicating a defect in tube formation or genome piloting. These proteins differed in the ability to compete with the wild-type H protein. When the wild type was allowed to assemble in the presence of Δ11-1 and Δ11-2 proteins, the two species were incorporated at approximately equal levels. As before, the resulting hybrid particles exhibited reduced infectivity. In contrast, only

the wild-type H protein was found in particles synthesized in the presence of the Δ7-10 and Δ14-10&11 proteins.

Tube length requirements and its evolution. A minimum tube length is likely required to span the cell wall. Compared to the wild-type structure, deletions of two heptads, one hendecad, or a single heptad would, respectively, shorten the 170-Å tube by approximately 18 Å, 16 Å, or 9 Å. The G80V mutation permitted Δ7-3 mutant protein incorporation into viable progeny, which reduces the minimum tube length to 161 Å. The assays used in these studies measure viability: ΔH proteins that fail to properly oligomerize cannot be distinguished from those too short to span the cell wall. Thus, the minimal tube length imposed by the host has not been precisely determined. The tube length required for infectivity could change throughout the course of evolution. If the cell wall became thicker, the virus would need to adapt by duplicating DNA encoding repeating motifs. Indeed, duplication events occurred during our studies: the Δ11-1 mutant duplicated a neighboring hendecad, restoring the protein to wild-type length.

Multiple functions likely require multiple structures. H protein must adopt at least two conformations during the viral life cycle. It is incorporated as a monomer during procapsid assembly and then oligomerizes into a tube during infection. As discussed above, both conformations can be perturbed by deleting a hendecad or heptad. It was previously demonstrated that efficient viral coat protein production requires *de novo* H protein synthesis (16), indicating that H plays another intracellular role in the viral life cycle independent of assembly. Thus, it is likely that H has a third conformation. Regardless of the incorporation and tube assembly defects, exogenous expression of each ΔH construct restored *am*(*H*) coat protein synthesis to wild-type levels, indicating that its ability to perform this third function has remained intact. The region(s) of the protein associated with this function has yet to be determined.

ACKNOWLEDGMENTS

We acknowledge S. M. Doore for discussions.

This research was supported by National Science Foundation grants MCB-1408217 (B.A.F.), U.S. Department of Agriculture Hatch funds to the University of Arizona, and the BIO5 Institute.

FUNDING INFORMATION

This work, including the efforts of Bentley A. Fane, was funded by National Science Foundation (NSF) (MCB 1408217).

REFERENCES

1. **Leiman PG, Shneider MM.** 2012. Contractile tail machines of bacteriophages, p 93–114. *In* Rossmann MG, Rao VG (ed), Viral molecular machines. Springer, New York, NY.
2. **Hu B, Margolin W, Molineux IJ, Liu J.** 2013. The bacteriophage t7 virion undergoes extensive structural remodeling during infection. Science **339:** 576–579. http://dx.doi.org/10.1126/science.1231887.
3. **Esquinas-Rychen M, Erni B.** 2001. Facilitation of bacteriophage lambda DNA injection by inner membrane proteins of the bacterial phosphoenolpyruvate:carbohydrate phosphotransferase system (PTS). J Mol Microbiol Biotechnol **3:**361–370.
4. **Russel M, Model P.** 2006. Filamentous phage, p 146–160. *In* Calendar R (ed), The bacteriophages, 2nd ed. Oxford Press, London, United Kingdom.
5. **Van Duin J, Tsareva N.** 2006. Single-stranded RNA phages, p 175–196. *In* Calendar R (ed), The bacteriophages, 2nd ed. Oxford Press, London, United Kingdom.
6. **Jazwinski SM, Lindberg AA, Kornberg A.** 1975. The gene H spike protein of bacteriophages phiX174 and S13. I. Functions in phage-receptor recognition and in transfection. Virology **66:**283–293.
7. **Jazwinski SM, Marco R, Kornberg A.** 1975. The gene H spike protein of bacteriophages phiX174 and S13. II. Relation to synthesis of the parenteral replicative form. Virology **66:**294–305.
8. **Sun L, Young LN, Zhang X, Boudko SP, Fokine A, Zbornik E, Roznowski AP, Moulineux I, Rossmann MG, Fane BA.** 2014. Icosahedral ΦX174 forms a tail for DNA transport. Nature **505:**432–435.
9. **Sun L, Rossmann MG, Fane BA.** 2014. High-resolution structure of a virally encoded DNA-translocating conduit and the mechanism of DNA penetration. J Virol **88:**10276–10279. http://dx.doi.org/10.1128/JVI.00291-14.
10. **Tang J, Lander GC, Olia AS, Li R, Casjens S, Prevelige P, Jr, Cingolani G, Baker TS, Johnson JE.** 2011. Peering down the barrel of a bacteriophage portal: the genome packaging and release valve in p22. Structure **19:**496–502. http://dx.doi.org/10.1016/j.str.2011.02.010.
11. **Olia AS, Prevelige PE, Jr, Johnson JE, Cingolani G.** 2011. Three-dimensional structure of a viral genome-delivery portal vertex. Nat Struct Mol Biol **18:**597–603. http://dx.doi.org/10.1038/nsmb.2023.
12. **Egelman EH, Xu C, DiMaio F, Magnotti E, Modlin C, Yu X, Wright E, Baker D, Conticello VP.** 2015. Structural plasticity of helical nanotubes based on coiled-coil assemblies. Structure **23:**280–289. http://dx.doi.org/10.1016/j.str.2014.12.008.
13. **Pieters BJ, van Eldijk MB, Nolte RJ, Mecinovic J.** 2016. Natural supramolecular protein assemblies. Chem Soc Rev **45:**24–39. http://dx.doi.org/10.1039/C5CS00157A.
14. **Cherwa JE, Jr, Organtini LJ, Ashley RE, Hafenstein SL, Fane BA.** 2011. In vitro assembly of the oX174 procapsid from external scaffolding protein oligomers and early pentameric assembly intermediates. J Mol Biol **412:**387–396. http://dx.doi.org/10.1016/j.jmb.2011.07.070.
15. **Cherwa JE, Jr, Uchiyama A, Fane BA.** 2008. Scaffolding proteins altered in the ability to perform a conformational switch confer dominant lethal assembly defects. J Virol **82:**5774–5780. http://dx.doi.org/10.1128/JVI.02758-07.
16. **Ruboyianes MV, Chen M, Dubrava MS, Cherwa JE, Jr, Fane BA.** 2009. The expression of N-terminal deletion DNA pilot proteins inhibits the early stages of phiX174 replication. J Virol **83:**9952–9956. http://dx.doi.org/10.1128/JVI.01077-09.
17. **Fane BA, Hayashi M.** 1991. Second-site suppressors of a cold-sensitive prohead accessory protein of bacteriophage phi X174. Genetics **128:** 663–671.
18. **Fane BA, Head S, Hayashi M.** 1992. Functional relationship between the J proteins of bacteriophages phi X174 and G4 during phage morphogenesis. J Bacteriol **174:**2717–2719.
19. **Bernhardt TG, Struck DK, Young R.** 2001. The lysis protein E of phi X174 is a specific inhibitor of the MraY-catalyzed step in peptidoglycan synthesis. J Biol Chem **276:**6093–6097. http://dx.doi.org/10.1074/jbc.M007638200.
20. **Sanger F, Coulson AR, Friedmann T, Air GM, Barrell BG, Brown NL, Fiddes JC, Hutchison CA, III, Slocombe PM, Smith M.** 1978. The nucleotide sequence of bacteriophage phiX174. J Mol Biol **125:**225–246. http://dx.doi.org/10.1016/0022-2836(78)90346-7.
21. **Fane BA, Shien S, Hayashi M.** 1993. Second-site suppressors of a cold-sensitive external scaffolding protein of bacteriophage phi X174. Genetics **134:**1003–1011.
22. **Burch AD, Ta J, Fane BA.** 1999. Cross-functional analysis of the Microviridae internal scaffolding protein. J Mol Biol **286:**95–104. http://dx.doi.org/10.1006/jmbi.1998.2450.
23. **Uchiyama A, Fane BA.** 2005. Identification of an interacting coat-external scaffolding protein domain required for both the initiation of phiX174 procapsid morphogenesis and the completion of DNA packaging. J Virol **79:**6751–6756. http://dx.doi.org/10.1128/JVI.79.11.6751-6756.2005.
24. **Cherwa JE, Jr, Sanchez-Soria P, Wichman HA, Fane BA.** 2009. Viral adaptation to an antiviral protein enhances the fitness level to above that of the uninhibited wild type. J Virol **83:**11746–11750. http://dx.doi.org/10.1128/JVI.01297-09.
25. **Hafenstein SL, Chen M, Fane BA.** 2004. Genetic and functional analyses of the øX174 DNA binding protein: the effects of substitutions for amino acid residues that spatially organize the two DNA binding domains. Virology **318:**204–213. http://dx.doi.org/10.1016/j.virol.2003.09.018.
26. **McKenna R, Bowman BR, Ilag LL, Rossmann MG, Fane BA.** 1996. Atomic structure of the degraded procapsid particle of the bacteriophage G4: induced structural changes in the presence of calcium ions and func-

tional implications. J Mol Biol **256:**736–750. http://dx.doi.org/10.1006/jmbi.1996.0121.
27. **Cherwa JE, Jr, Young LN, Fane BA.** 2011. Uncoupling the functions of a multifunctional protein: the isolation of a DNA pilot protein mutant that affects particle morphogenesis. Virology **411:**9–14. http://dx.doi.org/10.1016/j.virol.2010.12.026.
28. **Young LN, Hockenberry AM, Fane BA.** 2014. Mutations in the N terminus of the oX174 DNA pilot protein H confer defects in both assembly and host cell attachment. J Virol **88:**1787–1794. http://dx.doi.org/10.1128/JVI.03227-13.
29. **Mano Y, Sakai H, Komano T.** 1979. Growth and DNA synthesis of bacteriophage phi x174 in a dnaP mutant of Escherichia coli. J Virol **30:**650–656.
30. **Young R, Wang I-N.** 2006. Phage lysis, p 104–128. *In* Calendar R (ed), The bacteriophages, 2nd ed. Oxford Press, London, United Kingdom.
31. **Harbury PB, Zhang T, Kim PS, Alber T.** 1993. A switch between two-, three-, and four-stranded coiled coils in GCN4 leucine zipper mutants. Science **262:**1401–1407. http://dx.doi.org/10.1126/science.8248779.
32. **Bayer ME, Starkey TW.** 1972. The adsorption of bacteriophage phi X174 and its interaction with Escherichia coli; a kinetic and morphological study. Virology **49:**236–256. http://dx.doi.org/10.1016/S0042-6822(72)80026-6.
33. **Spindler KR, Hayashi M.** 1979. DNA synthesis in Escherichia coli cells infected with gene H mutants of bacteriophage phi X174. J Virol **29:**973–982.
34. **Dokland T, McKenna R, Ilag LL, Bowman BR, Incardona NL, Fane BA, Rossmann MG.** 1997. Structure of a viral procapsid with molecular scaffolding. Nature **389:**308–313. http://dx.doi.org/10.1038/38537.
35. **McKenna R, Xia D, Willingmann P, Ilag LL, Krishnaswamy S, Rossmann MG, Olson NH, Baker TS, Incardona NL.** 1992. Atomic structure of single-stranded DNA bacteriophage phi X174 and its functional implications. Nature **355:**137–143. http://dx.doi.org/10.1038/355137a0.